# CONCEALMENT OF TRANSMISSION ERRORS IN JPEG-2000 IMAGES USING ADAPTIVE LINEAR PREDICTION AND CROSSBAND INFORMATION

Shih-Hsiang Lin[#] and Jin-Jang Leou[#@]

# Department of Computer Science and Information Engineering, National Chung Cheng University
Chiayi, Taiwan 621, Republic of China
E-mail: jjleou@cs.ccu.edu.tw

## ABSTRACT

For entropy-coded JPEG-2000 images, a transmission error in a codeword (subband sample) may cause the underlining codeword (subband sample) and its subsequent codewords (subband samples) to be misinterpreted, resulting in a great degradation of the received images. In this study, the error concealment approach (using adaptive linear prediction and crossband information) to transmission errors in JPEG-2000 images is proposed. When JPEG-2000 images are decomposed into 6 wavelet levels (levels 0-5), the subband samples in the corrupted blocks of any subband on levels 3-5 are simply replaced by zeros. Adaptive linear prediction and crossband information are performed only on the 3 lower levels (0-2). Because the correlations between different subbands in horizontal and vertical directions are different, depending on (1) the position of the corrupted block, (2) the condition of correctly-received blocks in neighboring subbands, and (3) the statistical property (variance) of the corrupt block, the proposed approach adaptively selects one among 119 sets of linear prediction coefficients to conceal a corrupted block in the wavelet transform domain. Based on the simulation results obtained in this study, the proposed approach can recover high-quality JPEG-2000 images from the corresponding corrupted JPEG-2000 images.

Keywords: transmission error, JPEG-2000 image, adaptive lnear prediction, crossband information

## 1. INTRODUCTION

Because JPEG-2000 images are entropy-coded [1]-[2], a transmission error in a codeword (subband sample) may cause the underlining codeword (subband sample) and its subsequent codewords (subband samples) to be misinterpreted, resulting in a great degradation of the received images. Because each packet of JPEG-2000 image bitstream is ahead with a 3-byte *Resync* code (a synchronization codeword), after the decoder receives any synchronization codeword, the decoder will resynchronize the decoding operation regardless of the preceding slippage or transmission errors. Although the propagation effect of transmission errors can be confined within a packet, a transmission error will greatly degrade the quality of the received JPEG-2000 images, as an illustrated example shown in Fig. 1.

Most existing methods for transmission errors are developed for block-wise DCT-based compressed images [1], which may be classified into three main categories: (1) the channel coding approach [3], (2) the detection and correction approach [4], and (3) the detection and concealment approach [5]-[7]. On the other hand, the existing methods for transmission errors in wavelet-based compressed images may be classified into four categories: (1) the channel coding approach [8], (2) the priority error protection approach [9]-[10], (3) the robust entropy coding approach [11]-[12], and (4) the detection and concealment approach [13]-[14]. For the priority error protection approach, the more important data is given the higher protection. For the robust entropy coding approach, adding extra redundancy in the entropy-coding stage is used to detect transmission errors and/or prevent error propagation. For the detection and concealment approach, transmission errors are detected and concealed by using the crossband information and the relationship between subband coefficients.

Because the foregoing few error concealment methods for various DCT-based and wavelet-based images are not suitable for the JPEG-2000 images using the EBCOT coding algorithm. In this study, the error concealment approach using adaptive linear prediction and crossband information for JPEG-2000 image is proposed. Within the proposed approach, when JPEG-2000 images are decomposed into 6 wavelet levels (default levels 0-5), the subband samples in the corrupted blocks of any subband on levels 3-5 are simply replaced by zeroes. Adaptive linear prediction and crossband information are performed only on the 3 lower levels (0-2), or equivalently the 7 lower frequency subbands. Within the 3 lower levels, because the correlations between different subbands in horizontal and vertical directions are different, depending on (1) the position of the corrupted block, (2) the condition of correctly-received blocks in neighboring subbands,

+ : Workshop on Image Processing and Pattern Recognition.
@: Author to whom all correspondence should be addressed. Tel:886-5-2720411Ext.5310, Fax:886-5-2720859

and (3) the statistical property (variance) of the corrupt block, the proposed approach adaptively selects one among 119 sets of linear prediction coefficients to conceal a corrupted block in the wavelet transform domain.

Here a transmission error may be (1) a single bit error, or (2) a burst error. To simplify the processing steps in the proposed approach, a burst error containing several error bit segments is treated as several transmission errors, i.e., a transmission error is equivalently either a single bit error or a burst error containing N successive error bits. For simplicity, it is assumed that (1) *the Global Header* or *the Tile Header* containing the variance information about all the transmitted blocks is correctly-received, (2) the lowest subband $LL_0$ is correctly-received. The error concealment approach for the case that $LL_0$ is corrupted is developed in [15], which is omitted here. This paper is organized as follows. A brief overview of the JPEG-2000 compression standard and adaptive linear prediction is described in Section 2. The proposed concealment approach is addressed in Section 3. Simulation results are included in Section 4, followed by concluding remarks.

## 2. THE JPEG-2000 COMPRESSION STANDARD AND ADAPTIVE LINEAR PREDICTION

### 2.1 JPEG-2000 Compression Standard

The basic organization of a JPEG-2000 bitstream is shown in Fig. 2. JPEG-2000 decomposes an image into 6 resolution levels. Level 0 contains only one subband denoted by $LL_0$. Levels 1, 2, 3, 4, and 5 individually contain three subbands denoed by ($LH_l$, $HL_l$, $HH_l$), $l$ =1, 2, 3, 4, 5, respectively. Each "packet" contains all subbands on one resolution level (default). For level 0, only the subband $LL_0$ is included in the first packet, and for level $l$, where $l \geq 1$, the three subbands $LH_l$, $HL_l$, and $HH_l$ are together included in the $(l+1)th$ packet. That is, a JPEG-2000 bitstream will contain 6 packets (default). The JPEG-2000 coding technique, namely, EBCOT divides each subband into sample blocks $64 \times 64$ (default) in size. If the size of a subband is less than or equal to $64 \times 64$, the subband is just a block. For a JPEG-2000 image ($512 \times 512$ in size) decomposed into 6 levels (levels 0-5) will contain 6 separate packets, or equivalently 16 separate subbands, or equivalently 70 separate blocks.

For convenience, the seven low frequency subbands, $LL_0$, $LH_1$, $HL_1$, $HH_1$, $LH_2$, $HL_2$, and $HH_2$ are labeled by 0-6, respectively. In the following discussions, all normalized quantities, including normalized image samples, normalized subband samples, and normalized quantized subband samples, have been de-normalized to their original dynamic ranges.

### 2.2 Adaptive Linear Prediction

An adaptive linear prediction system [16] includes an adaptive input signal vector with elements $x_0, x_1, ..., x_L$, a corresponding set of adaptive weights, $w_0, w_1, ..., w_L$, and a summing unit $\sum$. The adaptive linear prediction can be given by: $y = \sum_{k=0}^{L} w_k x_k$. If $X$ denotes the input signal vector and $W$ denotes the corresponding adaptive weighted vector, i.e., $X = [x_0\ x_1 \ldots x_L]^T$, $W = [w_0\ w_1 \ldots w_L]^T$, where $X^T$ denotes the transpose of $X$, $y = W^T X$, and the elements of $W$ are adaptively determined by some adaptive mechanism.

## 3. PROPOSED APPROACH

In this study, it is assumed that whether a packet is corrupted or not has been determined by some error detection approach for JPEG-2000 images [15] and the synchronization codeword (*Resync* code) is included within the packet header. Based on the organization of JPEG-2000 bit-stream packet, the JPEG-2000 decoder can be translated as three decoding control procedures, namely, Decode_image, Decode_tile, and Decode_packet. The proposed error concealment approach is embedded within the Decode_packet control procedure.

### 3.1 Proposed Error Concealment Scheme for Subbands on Levels 3, 4, and 5

Because the values of all subband samples in any high frequency subband are around some constant, the variation between the subband samples in a block in any high frequency subband is not significant. Within the proposed error concealment approach, the subband samples in any corrupted block of any subbband on levels 3-5 are simply replaced by zeros.

### 3.2 Proposed Error Concealment Schemes for Subbands on Level 1

#### 3.2.1 Error concealment for corrupted subband $LH_1$ on level 1

When $LH_1$ is corrupted, there exist several cases to be discussed. Because $HL_1$ and $HL_2$ as well as all the subbands on levels 3-5 almost contribute no information for concealing $LH_1$, which are ignored in the proposed concealment schemes for $LH_1$.

**A. Only $LL_0$ is correctly-received (or equivalently $HH_1$, $LH_2$, and $HH_2$ are corrupted)**

If $LH_1$ is corrupted and only $LL_0$ is correctly-received, only the information in $LL_0$ can be used to conceal corrupted $LH_1$. Within the proposed approach, as shown in Fig. 3, the corrupted subband sample in $LH_1$ with wavelet coordinate $(a,b)$, $y^1_{a,b}$, is concealed by linearly weighted sum of 25 subband samples in the corresponding locations in $LL_0$, i.e.,

$$\hat{y}^1_{a,b} = w^0_{a-2,b-2}x^0_{a-2,b-2} + w^0_{a-2,b-1}x^0_{a-2,b-1} + w^0_{a-2,b}x^0_{a-2,b} + w^0_{a-2,b+1}x^0_{a-2,b+1} + w^0_{a-2,b+2}x^0_{a-2,b+2} + w^0_{a-1,b-2}x^0_{a-1,b-2} + w^0_{a-1,b-1}x^0_{a-1,b-1} + w^0_{a-1,b}x^0_{a-1,b} + w^0_{a-1,b+1}x^0_{a-1,b+1} + w^0_{a-1,b+2}x^0_{a-1,b+2} + \ldots + w^0_{a+2,b-2}x^0_{a+2,b-2} + w^0_{a+2,b-1}x^0_{a+2,b-1} + w^0_{a+2,b}x^0_{a+2,b} + w^0_{a+2,b+1}x^0_{a+2,b+1} + w^0_{a+2,b+2}x^0_{a+2,b+2} = \sum_{i=-2}^{2}\sum_{j=-2}^{2} w^0_{a+i,b+j}x^0_{a+i,b+j}, \quad (1)$$

where $\hat{y}^1_{a,b}$ is the concealed subband sample in $LH_1$ with wavelet coordinate $(a,b)$. The 25 weighting coefficients $\{w_{a-2,b-2},\cdots,w_{a+2,b+2}\}$ form a weighting coefficient vector for this case.

### B. $LL_0$, $LH_2$, and $HH_2$ are correctly-received (or equivalently $HH_1$ is corrupted)

In this case, a subband sample in correctly-received subband $LH_2$ can be further classified into a significant or non-significant subband sample. If the value of a subband sample is greater than some threshold $T_{sign}$, it is significant; otherwise, it is a non-significant . For a subband sample in $LH_1$, there are four corresponding subband sample in $LH_2$. In this study, a subband sample in $LH_1$ to be concealed is classified as a significant subband sample if any of the four corresponding subband samples in $LH_2$ is classified as a significant subband sample.

As shown in Fig. 4(a), the corrupted significant subband sample in $LH_1$ with wavelet coordinate $(a,b)$, $y^1_{a,b}$, is concealed by linearly weighted sum of 57 significant subband samples in the corresponding locations in $LL_0$, $LH_2$, and $HH_2$, i.e.,

$$\begin{aligned}\hat{y}^1_{a,b} = &\sum_{i=-1}^{1}\sum_{j=-1}^{1} w^0_{a+i,b+j}x^0_{a+i,b+j} + \\ &\sum_{i=2}^{2}(w^4_{2(a+i),2b}x^4_{2(a+i),2b} + w^4_{2(a+i),2b+1}x^4_{2(a+i),2b+1} + w^4_{2(a+i)+1,2b}x^4_{2(a+i)+1,2b} + w^4_{2(a+i)+1,2b+1}x^4_{2(a+i)+1,2b+1}) + \\ &\sum_{j=-1,1}(w^4_{2a,2(b+j)}x^4_{2a,2(b+j)} + w^4_{2a,2(b+j)+1}x^4_{2a,2(b+j)+1} + w^4_{2a+1,2(b+j)}x^4_{2a+1,2(b+j)} + w^4_{2a+1,2(b+j)+1}x^4_{2a+1,2(b+j)+1}) + \\ &\sum_{j=-1}^{1}(w^6_{2a,2(b+j)}x^6_{2a,2(b+j)} + w^6_{2a,2(b+j)+1}x^6_{2a,2(b+j)+1} + w^6_{2a+1,2(b+j)}x^6_{2a+1,2(b+j)} + w^6_{2a+1,2(b+j)+1}x^6_{2a+1,2(b+j)+1}) + \\ &\sum_{i=-1,1}(w^6_{2(a+i),2b}x^6_{2(a+i),2b} + w^6_{2(a+i),2b+1}x^6_{2(a+i),2b+1} + w^6_{2(a+i)+1,2b}x^6_{2(a+i)+1,2b} + w^6_{2(a+i)+1,2b+1}x^6_{2(a+i)+1,2b+1}). \quad (2)\end{aligned}$$

On the other hand, as shown in Fig. 4(b), the corrupted non-significant subband sample in $LH_1$ with wavelet coordinate $(a,b)$, $y^1_{a,b}$, is concealed by linearly weighted sum of 12 non-significant subband samples in the corresponding locations in $LH_2$, i.e.,

$$\hat{y}^1_{a,b} = \sum_{i=1}^{1}(w^4_{2(a+i),2b}x^4_{2(a+i),2b} + w^4_{2(a+i),2b+1}x^4_{2(a+i),2b+1} + w^4_{2(a+i)+1,2b}x^4_{2(a+i)+1,2b} + w^4_{2(a+i)+1,2b+1}x^4_{2(a+i)+1,2b+1}). \quad (3)$$

The 57 and 12 weighting coefficients form the two weighting coefficient vectors for concealing significant and non-significant subband samples in $LH_1$, respectively. Note that in Eqs. (2) and (3), $m = 0, 4, and\ 6$ in the symbol $x^m_{a,b}$ correspond to $LL_0$, $LH_2$, and $HH_2$, respectively, and the values of $w^m_{a,b}$ in Eqs. (2) and (3) for concealing significant and non-significant subband samples in $LH_1$ are distinct.

### C. $LL_0$, $HH_1$, $LH_2$, and $HH_2$ are correctly-received

Similar to case B ($LL_0$, $LH_2$, and $HH_2$ are correctly-received), the subband sample in correctly-received subband $LH_2$ as well as the corresponding subband sample in $LH_1$ to be concealed can be classified into a significant or non-significant subband sample by thresholding (with some threshold $T_{sign}$). Note that the thresholds $T_{sign}$ used in different cases may be distinct (depend on the variance of the correctly-received subband for making thresholding).

Within the proposed approach, as shown in Fig. 5(a), the corrupted significant subband sample in $LH_1$ with wavelet coordinate $(a,b)$, $y^1_{a,b}$, is concealed by linearly weighted sum of 62 significant subband samples in the corresponding locations in $LL_0$, $HH_1$, $LH_2$, and $HH_2$, i.e.,

$$\begin{aligned}\hat{y}^1_{a,b} = &\sum_{i=-1}^{1}\sum_{j=-1}^{1} w^0_{a+i,b+j}x^0_{a+i,b+j} + \sum_{j=-1}^{1} w^3_{a,b+j}x^3_{a,b+j} + \sum_{i=-1,1} w^3_{a+i,b}x^3_{a+i,b} + \\ &\sum_{i=2}^{2}(w^4_{2(a+i),2b}x^4_{2(a+i),2b} + w^4_{2(a+i),2b+1}x^4_{2(a+i),2b+1} + w^4_{2(a+i)+1,2b}x^4_{2(a+i)+1,2b} + w^4_{2(a+i)+1,2b+1}x^4_{2(a+i)+1,2b+1}) + \\ &\sum_{j=-1,1}(w^4_{2a,2(b+j)}x^4_{2a,2(b+j)} + w^4_{2a,2(b+j)+1}x^4_{2a,2(b+j)+1} + w^4_{2a+1,2(b+j)}x^4_{2a+1,2(b+j)} + w^4_{2a+1,2(b+j)+1}x^4_{2a+1,2(b+j)+1}) + \\ &\sum_{j=-1}^{1}(w^6_{2a,2(b+j)}x^6_{2a,2(b+j)} + w^6_{2a,2(b+j)+1}x^6_{2a,2(b+j)+1} + w^6_{2a+1,2(b+j)}x^6_{2a+1,2(b+j)} + w^6_{2a+1,2(b+j)+1}x^6_{2a+1,2(b+j)+1}) + \\ &\sum_{i=-1,1}(w^6_{2(a+i),2b}x^6_{2(a+i),2b} + w^6_{2(a+i),2b+1}x^6_{2(a+i),2b+1} + w^6_{2(a+i)+1,2b}x^6_{2(a+i)+1,2b} + w^6_{2(a+i)+1,2b+1}x^6_{2(a+i)+1,2b+1}). \quad (4)\end{aligned}$$

On the other hand, as shown in Fig. 5(b), the corrupted non-significant subband sample in $LH_1$ with wavelet coordinate $(a,b)$, $y^1_{a,b}$, is concealed by linearly weighted sum of 12 non-significant subband samples in the corresponding locations in $LH_2$, i.e.,

$$\hat{y}^1_{a,b} = \sum_{i=2}^{2}(w^4_{2(a+i),2b}x^4_{2(a+i),2b} + w^4_{2(a+i),2b+1}x^4_{2(a+i),2b+1} + w^4_{2(a+i)+1,2b}x^4_{2(a+i)+1,2b} + w^4_{2(a+i)+1,2b+1}x^4_{2(a+i)+1,2b+1}). \quad (5)$$

where $\hat{y}^1_{a,b}$ is the concealed subband sample in $LH_1$.

Note that the other cases for the corrupted subband $LH_1$ are treated as the degenerate cases of cases A, B, C. For example, for the corrupted subband $LH_1$, if the case is that $LL_0$, $HH_1$, and $LH_2$ are correctly-received (or equivalently $HH_2$ is corrupted), then the proposed approach uses the proposed concealment algorithms for case C, i.e., Eqs. (4) and (5), to conceal the subband samples of $LH_1$, where in Eqs. (4) and (5), all the subband samples from $HH_2$ are set to zeros.

Additionally, the similar concealment algorithms as that for the corrupted subband $LH_1$ are proposed for the corrupted subbands $HH_1$ and $HL_1$ on level 1, which are omitted here.

## 3.3 Proposed Error Concealment Schemes for Subbands on Level 2

As the illustrated case shown in Fig. 6, where $LL_0$ is correctly-received and any of the three subbands $LH_2$, $HL_2$, and $HH_2$ is corrupted, for a correctly-received subband samples $x^0_{a,b}$ in $LL_0$, there exist 4 corresponding "related" subband samples in a subband on level 2 to be concealed. In the proposed approach, the four "related" corrupted subband samples in a subband on level 2 will be concealed by linearly weighted sum of certain subband samples in their corresponding locations in related correctly-received subband(s) using four distinct weighting coefficient vectors. In this study, the four "related" subband samples in a subband on level 2 are concealed using four distinct weighting coefficient vectors.

### 3.3.1 Error concealment for corrupted subband

### $LH_2$ on level 2

When $LH_2$ is corrupted, there exist several cases to be discussed. Similarly, $HL_1$ and $HL_2$ as well as all the subbands on levels 3-5 almost contribute no information for concealing $LH_2$, which are ignored in the proposed concealment schemes for $LH_2$.

### A. Only $LL_0$ is correctly-received (or equivalently $LH_1$, $HH_1$, and $HH_2$ are corrupted)

In this case, because only the information in $LL_0$ can be used to conceal $LH_2$. Within this approach, as shown in Fig. 6, the corrupted subband sample in $LH_2$ with wavelet coordinate $(2a,2b)$, $y^4_{2a,2b}$ (the upper-left subband sample of the four "related" subband samples), is concealed by linearly weighted sum of 9 subband samples in the corresponding locations in $LL_0$, i.e.,

$$\begin{aligned}\hat{y}^4_{2a,2b} &= w^0_{a-1,b-1}x^0_{a-1,b-1} + w^0_{a-1,b}x^0_{a-1,b} + w^0_{a-1,b+1}x^0_{a-1,b+1} + \\ &\quad w^0_{a,b-1}x^0_{a,b-1} + w^0_{a,b}x^0_{a,b} + w^0_{a,b+1}x^0_{a,b+1} + \\ &\quad w^0_{a+1,b-1}x^0_{a+1,b-1} + w^0_{a+1,b}x^0_{a+1,b} + w^0_{a+1,b+1}x^0_{a+1,b+1} \\ &= \sum_{i=-1}^{1}\sum_{j=-1}^{1} w^0_{a+i,b+j}x^0_{a+i,b+j}, \end{aligned} \quad (6)$$

where $\hat{y}^4_{2a,2b}$ is the concealed subband sample in $LH_2$ with wavelet coordinate $(2a,2b)$. The other three "related" subband samples in $LH_2$, namely, $y^4_{2a+1,2b}$ (lower left), $y^4_{2a,2b+1}$ (upper right), and $y^4_{2a+1,2b+1}$ (lower right), can be similarly concealed by linearly weighted sum of 9 subband samples in the corresponding locations in $LL_0$ using distinct weighting coefficient vectors.

### B. $LL_0$, $LH_1$, and $HH_1$ are correctly-received (or equivalently $HH_2$ is corrupted)

For a subband sample in $LH_1$, there are four corresponding subband samples in the corrupted subband $LH_2$. In this study, the four corresponding ("related") subband samples in $LH_2$ to be concealed are all classified as significant subband samples if the corresponding subband sample in $LH_1$ is classified as a significant subband sample by thresholding (using the threshold $T_{sign}$ depending on the variance of $LH_1$).

As shown in Fig. 7(a), the corrupted significant subband sample in $LH_2$ with wavelet coordinate $(2a,2b)$, $y^4_{2a,2b}$ (the upper left subband sample of the four "related" subband samples), is concealed by linearly weighted sum of 19 significant subband samples in the corresponding locations in $LL_0$, $LH_1$, and $HH_1$, i.e.,

$$\begin{aligned}\hat{y}^4_{2a,2b} &= w^0_{a-1,b-1}x^0_{a-1,b-1} + w^0_{a-1,b}x^0_{a-1,b} + w^0_{a-1,b+1}x^0_{a-1,b+1} + \ldots + w^0_{a+1,b-1}x^0_{a+1,b-1} + w^0_{a+1,b}x^0_{a+1,b} + w^0_{a+1,b+1}x^0_{a+1,b+1} + \\ &\quad w^1_{a-2,b}x^1_{a-2,b} + w^1_{a-1,b}x^1_{a-1,b} + w^1_{a,b}x^1_{a,b} + w^1_{a+1,b}x^1_{a+1,b} + w^1_{a+2,b}x^1_{a+2,b} + \\ &\quad w^3_{a-1,b}x^3_{a-1,b} + w^3_{a,b-1}x^3_{a,b-1} + w^3_{a,b}x^3_{a,b} + w^3_{a,b+1}x^3_{a,b+1} + w^3_{a+1,b}x^3_{a+1,b} + \\ &= \sum_{i=-2}^{2} w^1_{a+i,b}x^1_{a+i,b} + \sum_{j=-1}^{1} w^3_{a,b+j}x^3_{a,b+j} + \sum_{i=-1,1} w^3_{a+i,b}x^3_{a+i,b}. \end{aligned} \quad (7)$$

On the other hand, as shown in Fig. 7(b), the non-significant subband sample in $LH_2$ with wavelet coordinate $(2a,2b)$, $y^4_{2a,2b}$ (upper-left) is concealed by linearly weighted sum of 10 non-significant subband samples in the corresponding locations in $LH_1$ and $HH_1$, i.e.,

$$\begin{aligned}\hat{y}^4_{2a,2b} &= w^1_{a-2,b}x^1_{a-2,b} + w^1_{a-1,b}x^1_{a-1,b} + w^1_{a,b}x^1_{a,b} + w^1_{a+1,b}x^1_{a+1,b} + w^1_{a+2,b}x^1_{a+2,b} + \\ &\quad w^3_{a-1,b}x^3_{a-1,b} + w^3_{a,b-1}x^3_{a,b-1} + w^3_{a,b}x^3_{a,b} + w^3_{a,b+1}x^3_{a,b+1} + w^3_{a+1,b}x^3_{a+1,b} \\ &= \sum_{i=-2}^{2} w^1_{a+i,b}x^1_{a+i,b} + \sum_{j=-1}^{1} w^3_{a,b+j}x^3_{a,b+j} + \sum_{i=-1,1} w^3_{a+i,b}x^3_{a+i,b}, \end{aligned} \quad (8)$$

where $\hat{y}^4_{2a,2b}$ is the concealed subband sample (upper left) in $LH_2$. Similar to case A, the other three "related" subband samples in $LH_2$ can be similarly concealed using distinct weighting coefficient vectors.

### C. $LL_0$, $LH_1$, $HH_1$, and $HH_2$ are correctly-received

For this case, as shown in Fig. 8(a), the corrupted significant subband sample in $LH_2$ with wavelet coordinate $(2a,2b)$, $y^4_{2q,2b}$ (upper left) is linearly weighted sum of 49 significant subband samples in the corresponding locations in $LL_0$, $LH_1$, $HH_1$, and $HH_2$, i.e.,

$$\begin{aligned}\hat{y}^4_{2a,2b} &= \sum_{i=-1}^{1}\sum_{j=-1}^{1} w^0_{a+i,b+j}x^0_{a+i,b+j} + \sum_{i=-2}^{2} w^1_{a+i,b}x^1_{a+i,b} + \sum_{j=-1}^{1} w^3_{a,b+j}x^3_{a,b+j} + \sum_{i=-1,1} w^3_{a+i,b}x^3_{a+i,b} + \\ &\quad \sum_{j=-1}^{1}(w^6_{2a,2(b+j)}x^6_{2a,2(b+j)} + w^6_{2a,2(b+j)+1}x^6_{2a,2(b+j)+1} + w^6_{2a+1,2(b+j)}x^6_{2a+1,2(b+j)} + w^6_{2a+1,2(b+j)+1}x^6_{2a+1,2(b+j)+1}) + \\ &\quad \sum_{i=-1,1}(w^6_{2(a+i),2b}x^6_{2(a+i),2b} + w^6_{2(a+i),2b+1}x^6_{2(a+i),2b+1} + w^6_{2(a+i)+1,2b}x^6_{2(a+i)+1,2b} + w^6_{2(a+i)+1,2b+1}x^6_{2(a+i)+1,2b+1}). \end{aligned} \quad (9)$$

On the other hand, as show in Fig. 8(b), the non-significant subband sample in $LH_2$ with wavelet coordinate $(2a,2b)$, $y^4_{2a,2b}$ (upper left), is concealed by linearly weighted sum of 15 non-significant subband samples in the corresponding locations in $LH_1$, $HH_1$, and $HH_2$, i.e.,

$$\begin{aligned}\hat{y}^4_{2a,2b} &= w^1_{a-2,b}x^1_{a-2,b} + w^1_{a-1,b}x^1_{a-1,b} + w^1_{a,b}x^1_{a,b} + w^1_{a+1,b}x^1_{a+1,b} + w^1_{a+2,b}x^1_{a+2,b} + \\ &\quad w^3_{a-1,b}x^3_{a-1,b} + w^3_{a,b-1}x^3_{a,b-1} + w^3_{a,b}x^3_{a,b} + w^3_{a,b+1}x^3_{a,b+1} + w^3_{a+1,b}x^3_{a+1,b} + \\ &\quad w^6_{2a-1,2b}x^6_{2a-1,2b} + w^6_{2a,2b-1}x^6_{2a,2b-1} + w^6_{2a,2b}x^6_{2a,2b} + w^6_{2a,2b+1}x^6_{2a,2b+1} + w^6_{2a+1,2b}x^6_{2a+1,2b} \\ &= \sum_{i=-2}^{2} w^1_{a+i,b}x^1_{a+i,b} + \sum_{j=-1}^{1} w^3_{a,b+j}x^3_{a,b+j} + \sum_{i=-1,1} w^3_{a+i,b}x^3_{a+i,b} + \sum_{j=-1}^{1} w^6_{2a,2b+j}x^6_{2a,2b+j} + \sum_{i=-1,1} w^6_{2a+i,2b}x^6_{2a+i,2b}, \end{aligned} \quad (10)$$

where $\hat{y}^4_{2a,2b}$ is the concealed subband sample (upper left) in $LH_2$. The other three "related" subband samples in $LH_2$ can be similarly concealed by using distinct weighting coefficient vectors.

Additionally, the similar error concealment algorithms as that for the corrupted subband $LH_2$ are proposed for the corrupted subbands $HH_2$ and $HL_2$ on level 2, which are also omitted here.

Note that the weighting coefficient vectors in the proposed error concealment schemes are adaptively adjusted by (1) the position of the corrupted block (in the wavelet transform domain), (2) the condition of correctly-received corresponding blocks in neighboring subbands, and (3) the statistical property (variance) of the corrupted block. The weighting coefficient vectors described in Eqs. (1)-(10) are adaptively adjusted by the former two properties. To use the third property, in this study, based on the value of the variance ($\sigma^2$) of the corrupted block, each weighting coefficient vector for a particular case of a corrupted block has three weighting coefficient sets. In particular, each weighting vector for a corrupted block in $HH_2$ has only two weighting coefficient sets. In this study, if $\sigma^2 \le T_1$, the weighting coefficient vector is a zero vector. For the two cases: $T_1 < \sigma^2 \le T_2$ and $T_2 < \sigma^2$,

the weighting coefficient vector is set to two distinct weighting coefficient sets, respectively.

As described in Eqs. (1)~(10), there exist 65 distinct weighting coefficient vectors. Additionally, based on the variance of the corrupted block, each weighting coefficient vector can be set to 3 distinct weighting coefficient sets (including a zero vector). Therefore, the proposed approach need to determine and store 118 distinct weighting coefficient sets. The 119 (including the zero vector without storing) distinct weighting coefficient sets are determined by supervised learning using 10 distinct images. The proposed error concealment approach is summarized as Fig. 10.

## 4. SIMULATION RESULTS

Five test images "Airplane," "Baboon," "Lenna," "Peppers," and "Boat" with different bit error rates (BER) and different average lengths of burst errors ($N_{ave}$) are used to evaluate the performance of the proposed approach. The peak signal noise ratio (PSNR) is employed in this study as the objective performance measure. The average length of burst errors $N_{ave}$ is defined as: $N_{ave} = \sum_{i=1}^{N} i \times P_i$, where $P_i$ is the probability of a burst error containing $i$ successive error bits with $\sum_{i=1}^{N} P_i = 1$.

In this study, for simplicity, $N$ (the maximum number of successive error bits of a burst error) is set to 5 and $N_{ave}$ will lie within the range (1,5).

In terms of the PSNR in dB, the performance comparison between the zero-substitution approach and the proposed concealment approach for the test image "Lenna" with bit rate = 0.4bpp is listed in Table 1. As subjective measure of the quality of the processed (reconstructed) images, the original image, the corrupted image, and the processed images by the zero-substitution approach and by the proposed concealment approach with bit rate = 0.4bpp, BER = 0.1%, and $N_{ave}$ = 2 for the test image "Lenna" are shown in Fig. 10.

## 5. CONCLUDING REMARKS

Based on the simulation results obtained in this study, several phenomena can be observed. (1) Under the same bit rate (bpp), BER, and the same corrupted condition, the more smooth the original image is, the higher PSNR (dB) the corresponding error concealment results have. (2) Under the same bit rate, BER, and the same corrupted condition, if the original image contains many texture areas (such as "Baboon"), the quality as well as the PSNR values of the processed JPEG-2000 images by the proposed error concealment approach are relatively degraded. (3) Under the same bit rate, BER, and the same corrupted condition, if the original image contains many edge information, the proposed error concealment approach will have the better PSNR gains over the "no error concealment" approach and the zero-substitution approach. (4) For the higher BER, the proposed error concealment approach have the better PSNR gains over the "no error concealment" approach. (5) Under the same bit rate and BER, the corrupted condition (i.e., the distribution of corrupted blocks over all the subbands on levels 1-5), the threshold $T_{edge}$ for significant/non-significant subband sample classification, and the two thresholds $T_1$ and $T_2$ of block variance for selecting appropriate weighting coefficient set will affect the processed results of the proposed error concealment approach. (6) Under the same bit rate and BER, a corrupted JPEG-2000 image with a larger $N_{ave}$ will usually produce the better processed images with the higher PSNRs. That is because under the same BER, the larger $N_{ave}$ will usually produce the smaller number of corrupted blocks if the distribution of the corrupted subband samples over levels 1-5 are similar. (7) Under the same bit rate, BER, and the same corrupted condition, if the original image contains many texture areas (such as "Baboon"), the proposed error concealment approach will have the smaller PSNR gains over the zero-substitution approach, in particular, when the bit rate is very low. That is because when the bit rate is very low, the values of subband samples in all subbands (except $LL_0$) are around some constant. The concealment results of the zero-substitution approach and the proposed approach are relatively similar.

Based on the simulation results obtained in this study, the proposed approach can recover high-quality JPEG-2000 images from the corresponding corrupted JPEG-2000 images.

## REFERENCES


[1] Y. Wang and Q. F. Zhu, "Error control and concealment for video communication: a review," *Proc. of the IEEE*, vol. 86, no. 5, pp. 974-997, 1998.

[2] ISO/IEC JTC1/SC29/WG1 N1422, "JPEG2000 Verification Model 5.2 (Technical Description)," 1999.

[3] A. Poli and L. Huguet, *Error Correcting Code*. Englewood Cliffs, NJ: Prentice Hall, 1992.

[4] Y. H. Han and J. J. Leou, "Detection and correction of transmission errors in JPEG images," *IEEE Trans. on Circuits and Systems for Video Tech.*, vol. 8, no. 2, pp. 221-231, 1998.

[5] Y. Wang, Q. F. Zhu, and L. Shaw, "Maximally smooth image recovery in transform coding," *IEEE Trans. on Commun.*, vol. 41, no. 10, pp. 1544-1551, 1993.

[6] M. Ghanbari and V. Seferidis, "Cell-loss concealment in ATM video codecs," *IEEE Trans. on Circuits and Systems for Video Tech.*, vol. 3, no. 3, pp. 238-247, 1993.

[7] M. Bystrom, V. Parthasarathy, and J. W. Modestino, "Hybrid error concealment schemes for broadcast video transmission over ATM networks," *IEEE Trans. on Circuits and Systems for Video Tech.*, vol. 9, no. 6, pp. 868-881, 1999.

[8] P. G. Sherwood and K. Zeger, "Error protection

for progressive image transmission over memoryless and fading channels," *IEEE Trans. on Commun.*, vol. 46, no. 12, pp. 1555-1559, 1998.

[9] H. Man, F. Kossentini, and M. J. T. Smith, "Robust EZW image coding for noisy channels," *IEEE Signal Processing Letters*, vol. 4, no. 8, pp. 227-229, 1997.

[10] H. Man, F. Kossentini, and M. J. T. Smith, "A family of efficient and channel error resilient wavelet/subband image coders," *IEEE Trans. on Circuits and Systems for Video Tech.*, vol. 9, no. 1, pp. 95-108, 1999.

[11] J. C. Liu, W. L. Hwang, W. J. Hwang, and M. S. Chen, "Robust image compression based on EZW," in *Proc. of 1998 IPPR Conf. on Computer Vision, Graphics, and Image Processing (CVGIP'98)*, Taipei, Taiwan, 1998, pp. 61-67.

[12] S. Whitehouse and N. Kingsbury, "The error resilient entropy code applied to zerotree coded image data," in *Proc. of IEEE 3rd Workshop on Multimedia Signal Processing*, 1999, pp. 425-430.

[13] K. Cinkler and K. D. Kammeyer, "Error correcting source decoding," *IEEE Signal Processing Letters*, vol. 6, no. 9, pp. 233-235, 1999.

[14] S. S. Hemami and R. M. Gray, "Subband-coded image reconstruction for lossy packet networks," *IEEE Trans. on Image Processing*, vol. 6, no. 4, pp. 523-539, 1997.

[15] M. C. Wu, "Detection and concealment of transmission errors in JPEG-2000 images," *Master Thesis*, Department of Computer Science and Information Engineering, National Chung Cheng University, Chiayi, Taiwan, R.O.C., 2000.

[16] B. Widrow and S. D. Stearns, *Adaptive Signal Processing*. Englewood Cliffs, NJ: Prentice Hall, 1985.

(a) (b)

Fig. 1. The original and corrupted JPEG-2000 images of "Lenna" with bit rate = 0.5bpp and bit error rate = 0.3%: (a) the original image; (b) the corrupted image.

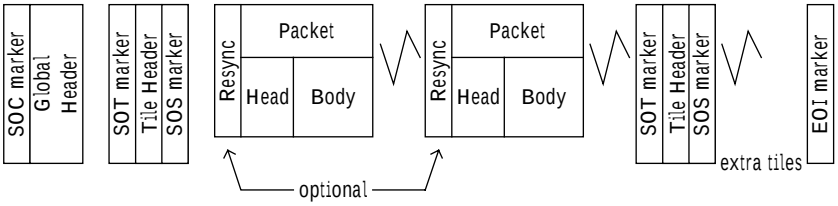


Fig. 2. Basic organization of a JPEG-2000 bitstream.

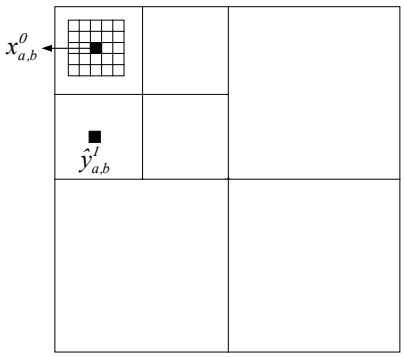


Fig. 3. The relationship between the subband samples in correctly-received $LL_0$ and a concealed subband sample in a corrupted subband $LH_1$.

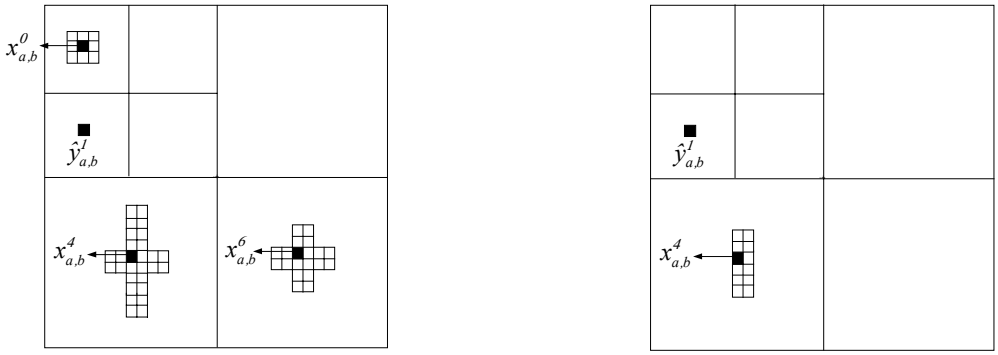


(a) significant subband samples (b) non-significant subband samples

Fig. 4. The relationship between the subband samples in correctly-received $LL_0$, $LH_2$, and $HH_2$ and a concealed subband sample in a corrupted subband $LH_1$.

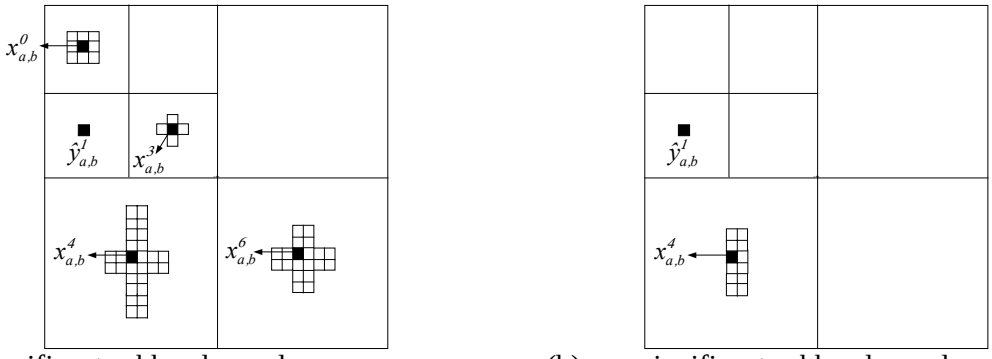


(a) significant subband samples (b) non-significant subband samples

Fig. 5. The relationship between the subband samples in correctly-received $LL_0$, $HH_1$, $LH_2$, and $HH_2$ and a concealed subband samples in a corrupted subband $LH_1$.

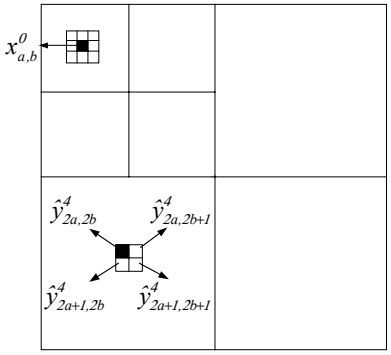


Fig. 6. The relationship between the subband samples in correctly-received $LL_0$ and a concealed subband sample in a corrupted subband $LH_2$.

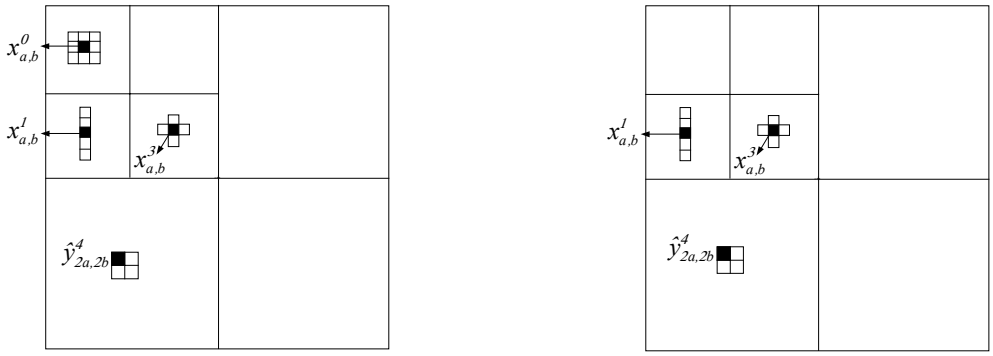


(a) significant subband samples (b) non-significant subband samples

Fig. 7. The relationship between the subband samples in correctly-received $LL_0$, $LH_1$, and $HH_1$ and a concealed subband sample in a corrupted subband $LH_2$.

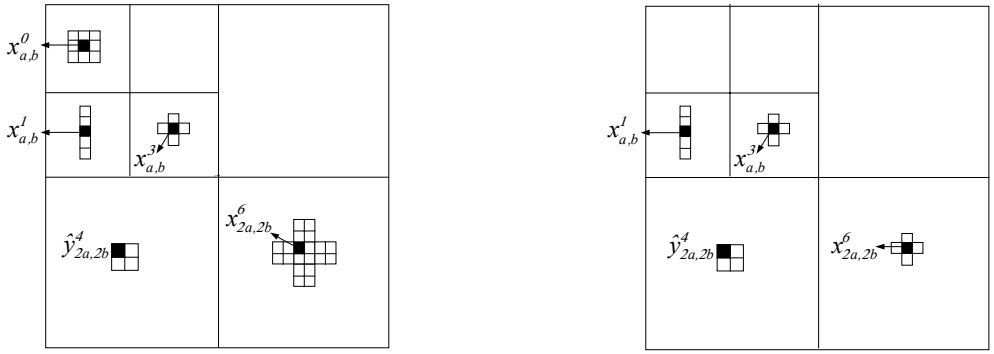


(a) significant subband samples (b) non-significant subband samples

Fig. 8. The relationship between the subband samples in correctly-received $LL_0$, $LH_1$, $HH_1$ and $HH_2$ and a concealed subband sample in a corrupted subband $LH_2$.

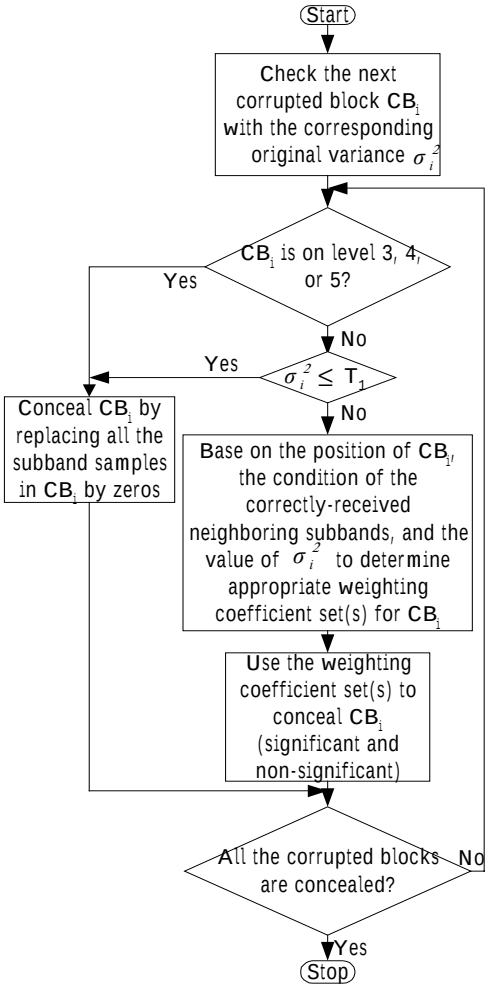


Fig. 9. The proposed error concealment approach.

Table 1. The simulation results PSNR (dB) for the case that errors only occur in subbands on level 2 (or equivalently $LH_2$, $HL_2$, and $HH_2$) and all the other subbands are correctly-received of the image "Baboon" with bit rate = 0.4bpp.

| BER | $N_{ave}$ | PSNR (dB) | | | |
|---|---|---|---|---|---|
| | | No loss | Corrupted | Zero-Sub. | Proposed |
| 0.02 % | 1 | 36.14 | 23.94 | 25.38 | 27.58 |
| | 2 | 36.14 | 23.97 | 26.76 | 30.82 |
| | 3 | 36.14 | 26.30 | 27.04 | 30.12 |
| | 4 | 36.14 | 26.25 | 26.57 | 30.12 |
| | 5 | 36.14 | 27.46 | 29.36 | 30.12 |
| 0.05 % | 1 | 36.14 | 27.11 | 29.36 | 30.12 |
| | 2 | 36.14 | 23.78 | 25.38 | 27.58 |
| | 3 | 36.14 | 27.44 | 31.45 | 31.45 |
| | 4 | 36.14 | 25.97 | 27.04 | 30.12 |
| | 5 | 36.14 | 27.46 | 29.36 | 29.82 |
| 0.1 % | 1 | 36.14 | 27.11 | 30.40 | 31.54 |
| | 2 | 36.14 | 25.78 | 29.36 | 29.82 |
| | 3 | 36.14 | 27.44 | 30.45 | 30.64 |
| | 4 | 36.14 | 25.97 | 29.36 | 29.82 |
| | 5 | 36.14 | 27.70 | 29.36 | 29.82 |
| 0.2 % | 1 | 36.14 | 20.06 | 25.38 | 27.58 |
| | 2 | 36.14 | 22.13 | 25.38 | 27.59 |
| | 3 | 36.14 | 24.51 | 26.10 | 30.82 |
| | 4 | 36.14 | 26.42 | 27.04 | 30.12 |
| | 5 | 36.14 | 28.32 | 29.36 | 29.82 |
| 0.5 % | 1 | 36.14 | 19.70 | 25.38 | 27.58 |
| | 2 | 36.14 | 17.55 | 25.38 | 27.58 |
| | 3 | 36.14 | 19.36 | 25.38 | 27.58 |
| | 4 | 36.14 | 23.02 | 26.10 | 30.82 |
| | 5 | 36.14 | 23.19 | 26.13 | 30.12 |

(a) (b) (c) (d)

Fig. 10. The original, corrupted, and processed test images of "lenna" with bit rate = 0.4bpp, BER = 0.1%, $N_{ave}$ = 2, and errors occur in $LH_1$, and $HH_1$: (a) the original image (PSNR = 36.14dB); (b) the corrupted image (PSNR = 21.02dB); (c)-(d) the processed image by the zero-substitution approach (PSNR = 22.82dB) and by the proposed concealment approach (PSNR = 26.30dB).